Shear-Friction Strength of RC Walls with 550 MPa Bars

Jang-woon Baek & Hong-gun Park

Seoul National University, Seoul, South Korea.

ABSTRACT: For low-rise walls with aspect ratio less than 0.5, which are commonly used in nuclear power plants, sliding failure is the critical issue in the shear design of the walls under repeated earthquake loading. The present study focused on the applicability of high strength bars to the shear-friction design of reinforced concrete walls. Low-rise walls (aspect ratio =0.33 and 0.5) with Grade 550 MPa bars were tested, to investigate the shear-friction strength under cyclic loading. The test parameters were shear reinforcement ratio, axial compressive loading, shear friction bars, and surface conditions of wall-foundation interface (groove construction joint or smooth flat joint). The test results showed that when smooth flat interface was used without groove joint, the specimens failed due to sliding at the interface. The test strength was significantly less than the shear friction strength of ACI 349. The use of shear friction bars increased the peak strength, but the peak strength did not reach the shear friction strength. On the other hand, in the case of walls with groove construction joint, shear friction failure was prevented.

1 INTRODUCTION

In the construction of nuclear power plants, a number of large diameter reinforcing bars are used in massive reinforced concrete (RC) walls, which significantly affects the constructability and economy. Thus, to enhance the constructability and economy, the use of high strength 550 MPa bars needs to be considered.

Park et al.[1] studied the use of Grade 550 MPa bars for the shear design of low-rise walls (aspect ratio h_w/l_w =1.0). In the study, the behavior of walls with Grade 550 MPa had no significant difference with that of Grade 420 MPa bars, in terms of failure mode, shear strength, ductility, and average diagonal shear crack width. Therefore, they reported that Grade 550 MPa bars are applicable to shear reinforcement for heavily reinforced low-rise walls.

On the other hand, shear-friction strength at wall-foundation interface is the critical issue for shear design of walls with aspect ratio h_w/l_w of walls lower than 1.0. In nuclear power plant structures, the majority of the walls have aspect ratios h_w/l_w less than 0.5. In this case, sliding failure can occur at the wall-foundation interface, which significantly decreases the shear capacity. Thus, in the design of short walls, to prevent sliding failure, shear-friction reinforcement is placed at the wall-foundation interface. According to existing results of shear friction test[2], shear-friction capacity in a cold joint decreases when high-strength bars are used for the shear-friction reinforcement. However, test results of shear friction capacity of walls with high strength bars have not been reported.

In the present study, cyclic lateral loading tests were performed for walls (h_w/l_w =0.33 and 0.5) with Grade 420 and 550 MPa bars, to investigate the shear-friction strength. The test parameters were the grade and ratio of shear reinforcement, axial compression, shear friction bars, and conditions of wall-foundation interface (groove construction joint or smooth flat surface). The test results were compared with the shear-friction strengths predicted by current design codes.

2 EXPERIMENTAL PROGRAM

2.1 Test specimens

The tests were performed for walls with two aspect ratios: 1) h_w/l_w= 0.5: 1500 mm (length) x 750 mm (height) x 200 mm (thickness), and 2) h_w/l_w =0.33: 1500 mm (length) x 500 mm (height) x 200 mm (thickness) (see **Fig. 1**).

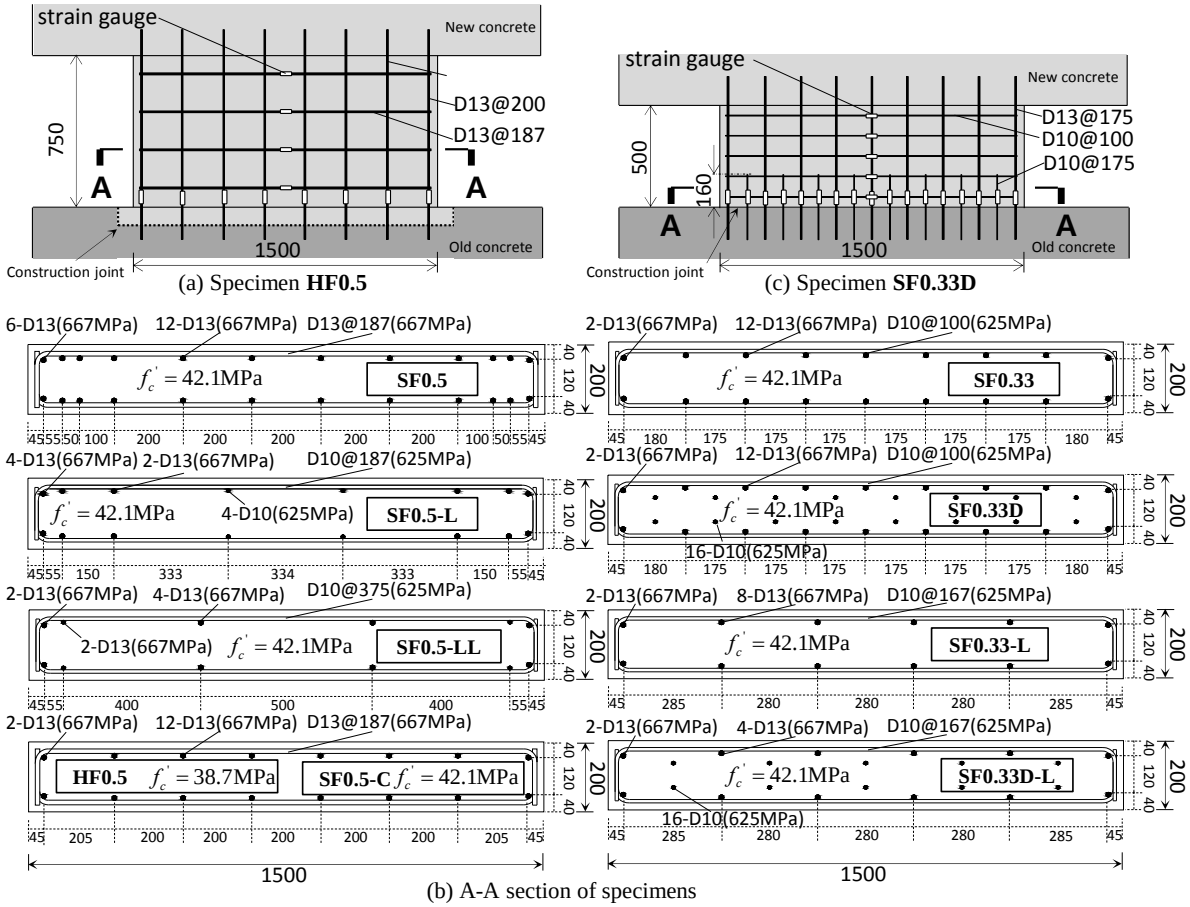

Figure 1. Dimensions and reinforcement details of specimens

Table 1. Design parameters of test specimens

Specimens	h_w /l_w	Concrete strength f_c' MPa [Compressive load, kN]	Web region								Boundary region		V_{sf} /V_f
			Horizontal bar				Vertical bar		Shear-friction bar		Vertical bar		
			V_s / V_{smax}	f_{yh} MPa	ρ_h (%)	$\rho_h f_{yh}$ MPa	f_{yv} MPa	ρ_v (%)	f_{ysf} MPa	ρ_{sf} (%)	f_{yf} MPa	ρ_f (%)	
SF0.5	0.5	42.1 [0]	1.04	667	0.68	4.51	667	0.69	-	-	667	1.90	0.98
SF0.5-L		42.1 [0]	0.55	625	0.38	2.38	667/ 625	0.33	-	-	667	1.69	0.92
SF0.5-LL		42.1 [0]	0.27	625	0.19	1.19	667	0.21	-	-	667	1.32	0.90
SF0.5-C		42.1 [882]	1.04	667	0.68	4.51	667	0.58	-	-	667	1.27	1.04
HF0.5		38.7 [735]	1.09	667	0.68	4.51	667	0.58	-	-	667	1.27	1.45
SF0.33	0.33	42.1 [0]	1.03	625	0.71	4.46	667	0.68	-	-	667	1.27	0.69
SF0.33-L		42.1 [0]	0.62	625	0.43	2.67	667	0.39	-	-	667	1.27	0.65
SF0.33D		42.1 [0]	1.03	625	0.71	4.46	667	0.68	625	0.38	667	1.27	1.01
SF0.33D-L		42.1 [0]	0.62	625	0.43	2.67	667	0.39	625	0.24	667	1.27	0.94

In Specimen **SF0.5** (h_w/l_w =0.5) (**Fig. 1(b)**), two layers of D13 Grade 550 MPa bars were used for horizontal and vertical reinforcement. The horizontal bar ratio ρ_h was 0.68% (**Table 1**), which is the permissible maximum bar ratio in accordance with ACI 349[3] (or ACI 318[4]). The flexural strength V_f of the specimen was designed to be equal to the shear strength V_n, following the design provisions and practice for RC walls. The flexural strength V_f was calculated by sectional analysis. The web vertical bar ratio ρ_v was 0.69%. Additional flexural bars were placed at the wall edges to attain the flexural strength: ρ_f= 1.9% (reinforcement ratio in wall boundary area). The shear-friction strength V_{sf} was close to the flexural strength V_f ($\fallingdotseq$ the shear strength V_n): V_{sf} / V_f = 0.98 (**Table 1**). The shear-friction strength was calculated in accordance with ACI 349 (or ACI 318), by using the smooth interface condition: the

friction coefficient μ = 0.6.

In Specimens **SF0.5-L** and **SF0.5-LL** (**Fig**. **1(b)**), the horizontal and vertical bar ratios were decreased to almost a half and quarter of those of Specimen **SF0.5**, respectively. The flexural strength V_f was the same as the shear strength V_n. On the other hand, the shear-friction strength was slightly less than the shear demand (i.e. the flexural strength): V_{sf} / V_f = 0.92 (**SF0.5-L**), and V_{sf} / V_f = 0.90 (**SF0.5-LL**).

In Specimen **SF0.5-C** (**Fig**. **1(b)**), axial compression (0.07 $A_c f_c'$) was applied at the top of the wall. The other details were identical to those of **SF0.5**, except for the flexural bars at the wall edges: the number of flexural bars were decreased considering the effect of axial compression. The shear-friction strength V_{sf} was close to the shear demand (i.e. the flexural strength V_f): V_{sf} / V_f = 1.04.

In Specimen **HF0.5** (**Figs**. **1(a)** and **(b)**), using a pocket metal form around the wall bottom, the construction joint was intentionally moved toward the inside of the foundation, to avoid sliding at the wall-foundation interface. Thus, the coefficient of shear friction capacity was increased to μ = 1.4, considering the monolithic interface. Thus, the shear-friction prediction V_{sf} was significantly increased to 2,921 kN. However, according to the permissible maximum one, the shear-friction strength was limited to V_{sf} = 1919 kN: V_{sf} / V_f= 1.45. The other details were identical to those of **SF0.5-C**.

In the case of walls with h_w/l_w = 0.5, the shear-friction strength V_{sf} was close to the flexural strength V_f. Thus, shear friction reinforcement was not required. In the case of walls with h_w/l_w = 0.33, on the other hand, the shear friction demand increased due to the reduced wall height. Thus, to prevent sliding failure, additional vertical bars for shear friction reinforcement were placed.

In Specimen **SF0.33** (**Fig**. **1(b)**), the shear friction strength was designed to be smaller than the flexural strength to measure accurate shear friction capacity by inducing shear friction failure. Thus, the ratio of the shear friction strength to the flexural strength was significantly decreased: V_{sf} / V_f = 0.69. Like **SF0.5**, the permissible maximum shear bar ratio was used for shear reinforcement: ρ_h= 0.71%, ρ_v= 0.68%, and ρ_f = 1.27%. In **SF0.33-L** (**Fig**. **1(b)**), the horizontal and vertical bar ratios were decreased to amost half of those of **SF0.33**: ρ_h= 0.43%, ρ_v= 0.39%, and ρ_f = 1.27%.

In Specimens **SF0.33D** and **SF0.33D-L** (**Figs**. **1(b)** and **(c)**), additional shear friction bars were placed so that the shear-friction strength was close to the flexural strength. For the shear friction bars, eight and five U-type bars were distributed along the wall section of **SF0.33D** (ρ_{sf} =0.38%) and **SF0.33D-L** (ρ_{sf} =0.24%) (**Table 1**), respectively. Consequently, the shear-friction strength was close to the flexural strength: V_{sf} / V_f = 1.01 for **SF0.33D** and 0.94 for **SF0.33D-L**.

In all the specimens, the concrete compressive strength was 42.1 MPa, except for 38.7 MPa in **HF0.5** (**Table 1**).

2.2 **Test procedure and instrumentation**

An axial compressive load and a cyclic lateral load were applied using the test set-up shown in **Fig. 2**. An axial load of approximately 0.07 $A_c f_c'$ (i.e. 882 kN in the case of 42.1 MPa concrete) was applied at the top of the wall by a displacement-controlled actuator. The level of the axial compressive force was maintained during cyclic lateral loading, by automatically controlling the vertical displacement.

The lateral loading protocol followed the "Acceptance Criteria for Special Structural Walls"[5], as shown in **Fig. 3**. **Fig. 2** shows the LVDTs for the measurement of lateral displacements, flexural deformations, shear deformations, and sliding at the base. **Figs. 1(a)** and **(b)** show the strain gauges, to measure the strains of the flexural and web vertical shear bars, horizontal bars, and shear-friction bars.

3 **TEST RESULT**

3.1 **Failure mode**

Fig. 4 shows the damages of the specimens at the end of tests. In the case of **SF0.5**, **SF0.5-L**, **SF0.5-LL**, and **SF0.5-C** [**Fig. 4(a)** to **(d)**]), although shear friction bars were not required in the design, unlike the expectation, sliding failure occurred at the wall-foundation interface (**SF** mode). The failure mode was the same as that of **SF0.33** and **SF0.33-L** [**Fig. 4(f)** and **(g)**] which were intentionally designed for sliding failure.

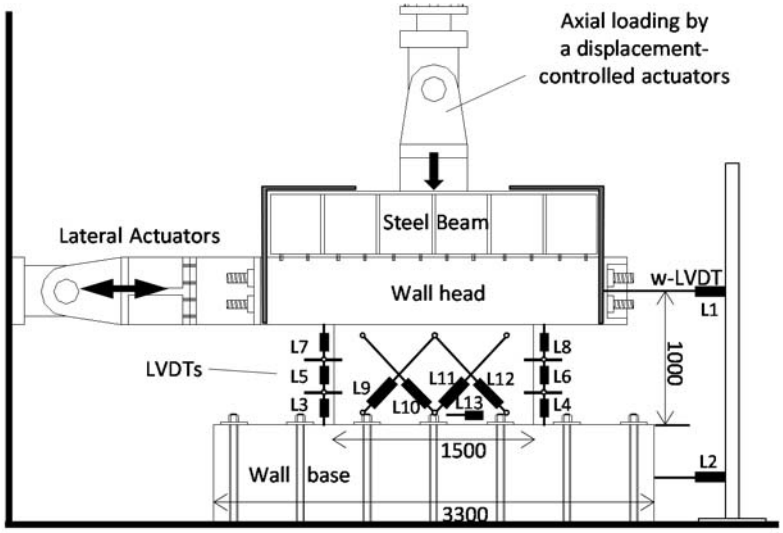

Figure 2. Test set-up

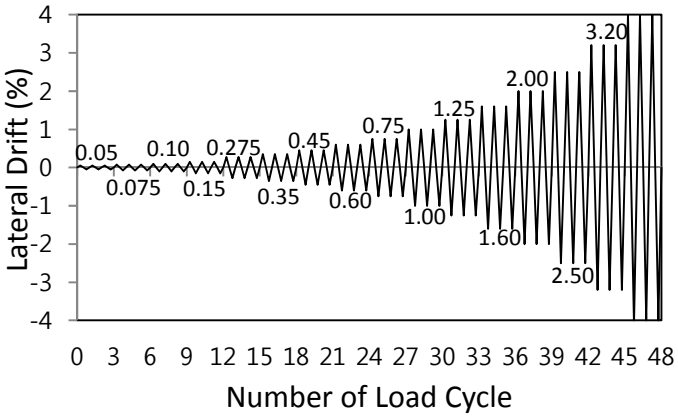

Figure 3. Lateral loading protocol

In Specimens **SF0.33D** and **SF0.33D-L** [**Fig. 4(h)** and **(i)**], despite the use of shear-friction bars, sliding failure occurred. The failure surface was formed along the end of the shear friction bars at a third of the wall height (167 mm above the wall-foundation interface) (**SW** mode).

In **HF0.5** with a groove construction joint, on the other hand, sliding failure was successfully prevented, and a mixed failure mode of shear and flexure occurred: crushing in the compression zone and diagonal tension cracking in the tension zone (**CC+DT** mode). **Table 2** summarizes the failure modes.

In **SF** mode specimens (**SF0.5**, **SF0.5-L**, **SF0.5-LL**, **SF0.5-C**, **SF0.33**, and **SF0.33-L**), horizontal splitting tensile cracking occurred at the wall-foundation interface and propagated wider as the load increased. Concrete spalling occurred near the wall-foundation interface and the vertical bars were exposed. Ultimately, sliding failure occurred along the cold joint. In **SF0.5-L** and **SF0.5-LL** with a half and quarter of the bar ratio of **SF0.5**, respectively, sliding occurred earlier. The number of cracks were smaller than that of **SF0.5**. On the other hand, in **SF0.5-C**, sliding was restrained by the compressive load ($0.07A_c f_c'$). In **SF0.33** and **SF0.33-L** with the lower aspect ratio, splitting cracks were concentrated at the interface, and sliding occurred earlier than that of **SF0.5** and **SF0.5-L.**

In **SW** mode specimens (**SF0.33D**, and **SF0.33D-L**), diagonal cracking occurred at the initial loading and spread over the entire wall panel. As the load increased, flexural cracking initiated at the location of the shear friction bar end, and the crack width notably increased. At the maximum load, a new horizontal crack parallel to the wall-foundation interface was generated at the height of wall center, and sliding along the horizontal crack occurred.

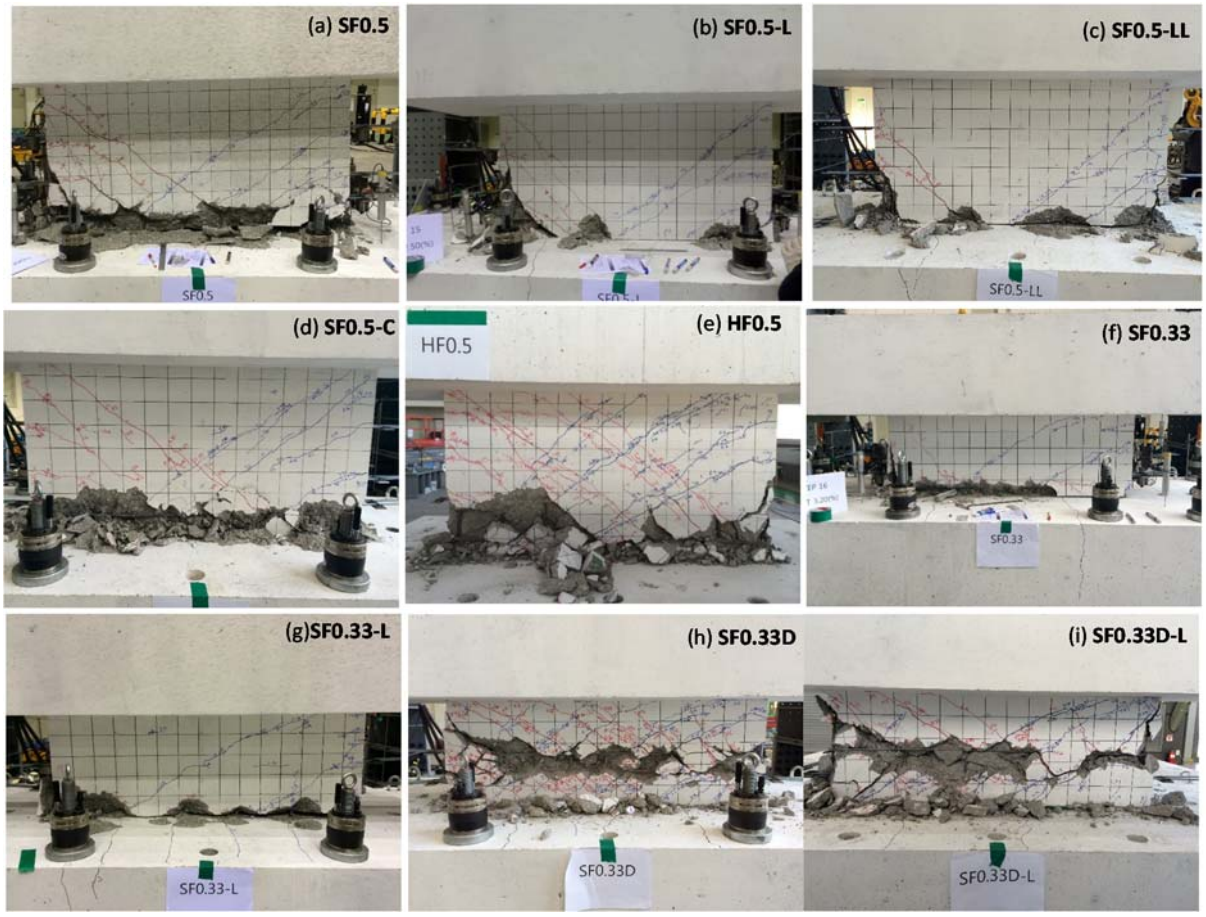

Figure 4. Failure modes of specimens at the end of test

Table 2. Strengths of test specimens and predictions by current design codes

Specimen	Aspect ratio h_w/l_w	Test results			Ratio of test strength to predictions		
		V_{test} kN	Drift at V_{test} %	Failure mode	ACI 349 shear friction provision V_{test} / V_{sf}	ACI 349 flexural provision V_{test} / V_f	Eurocode 2 shear friction provision V_{test} / V_{ni}
SF0.5	0.5	787	+0.45/-0.60	SF	0.65	0.63	0.62
SF0.5-L		497	+0.35/-0.60		0.70	0.64	0.64
SF0.5-LL		423	+0.28/-0.60		0.83	0.75	0.74
SF0.5-C		1087	+1.00/-1.00		0.81	0.84	1.25
HF0.5		1404	+0.85/-1.00	DT+CC	0.73	1.06	1.03
SF0.33	0.33	646	+0.35/-0.50	SF	0.71	0.49	0.66
SF0.33-L		421	+0.45/-0.20		0.69	0.45	0.63
SF0.33D		1045	+1.00/-0.60	SW	0.78	0.79	0.75
SF0.33D-L		726	+1.00/-0.60		0.83	0.78	0.78

Notes: V_f = flexural strength predictions, V_{test} = average value of the measured maximum loads in positive and negative loading directions, and V_{sf} and V_{sf} = shear-friction predictions provided by the provision of ACI 349 and Eurocode 2, respectively. SF is sliding failure at wall-foundation interface, DT is diagonal tension failure, CC is concrete crushing failure, and SW is sliding failure at wall center.

In **CC+DT** mode specimen (**HF0.5**), diagonal cracking gradually propagated over the entire wall panel. As the load increased, the width of the diagonal shear cracks increased and concrete spalling occurred at the bottom of the wall edges. Ultimately, concrete crushing occurred in the compression zone and diagonal tension cracking occurred in the tension zone.

3.2 **Lateral load-displacement relationships**

Fig. 5 shows the lateral load-displacement (lateral drift ratio) relationships of the test specimens. The

lateral displacement indicates the net displacement (L1-L2 in **Fig. 2**), excluding sliding of the wall base (L2 in **Fig. 2**). **Fig. 5** also shows the shear strength V_n, flexural strength V_f, and shear friction strength V_{sf} predicted by ACI 349 (ACI 318). In all the specimens except **HF0.5**, the peak strength did not reach the flexural strength V_f, which indicates that the measured maximum lateral load V_{test} was determined by shear failure before flexural yielding (**Figs. 6(a)** to **(d)** and **(f)** to **(i)**). On the other hand, in **HF0.5**, the peak strength was close to the flexural strength, showing flexural yielding (**Fig. 6(e)**). The flexural strength V_f was calculated by sectional analysis considering the effect of axial load.

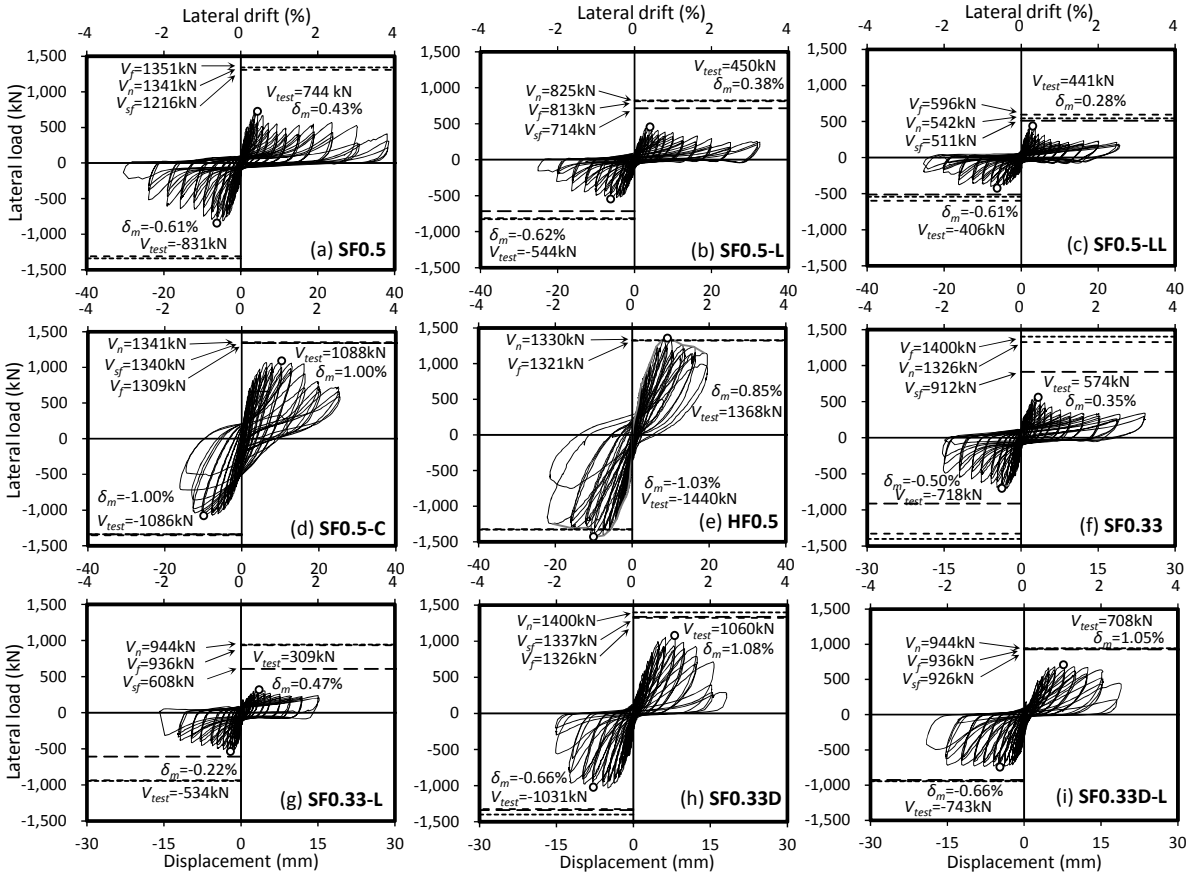

Figure 5. Lateral load-displacement relationships of specimens

In Specimen **SF0.5** (**Fig. 6(a)**) with Grade 550 MPa web bars (f_{yh} and f_{yv} =667 MPa, ρ_h=0.68%, ρ_v =0.69%, ρ_f =1.9%, and $\rho_h f_{yh}$ =4.50 MPa), the peak strength occurred at the drift ratio of +0.45 and -0.6%. The maximum strength V_{test} was +744 and -831 kN in the positive and negative loading directions, respectively, which was only 65% of the ACI 349 shear friction strength.

In **SF0.5-L** and **SF0.5-LL** (**Figs. 6(b)** and **(c)**) with smaller bar ratios, the maximum strength V_{test} and lateral drift decreased: in **SF0.5-L** (a half bar ratio), +450 and -544 kN at the drift ratio of +0.35 and -0.60%, and in **SF0.5-LL** (a quarter bar ratio), +441 and -406 kN at the drift ratio of +0.28 and -0.60%. However, the safety margin (i.e. the ratio of the test maximum strength to ACI 349 shear friction strength) was increased to 0.70 and 0.83 in **SF0.5-L** and **SF0.5-LL**, respectively, which implies that the ACI shear friction strength is more unsafe in higher bar ratios.

In **SF0.5-C** (**Fig. 6(d)**) subjected to axial compression loading, the maximum strength V_{test} and lateral drift were significantly increased: +1088 and -1086 kN at the drift ratios of +1.0 and -1.0%. However, the maximum strength did not reach the shear friction prediction: V_{test} / V_{sf} = 0.81.

In **HF0.5** (**Fig. 6(e)**) with groove construction joint and axial compression loading (**Fig. 1(a)**), the maximum strength V_{test} exceeded the flexural strength V_f: +1368 and -1440 kN at the drift ratio of +0.85

and -1.0%, showing ductile behavior until the +2.0 and -2.0% drift ratio.

In **SF0.33** (**Fig. 6(f)**) with aspect ratio h_w/l_w = 0.33 (f_{yh} =620 MPa, ρ_h=0.71%, f_{yv}=667MPa, ρ_v =0.68%, $\rho_h f_{yh}$=4.45 MPa, and ρ_f =1.27%), the maximum strength and drift ratio were smaller than those of **SF0.5**: +574 and -718 kN at the drift ratio of +0.35 and -0.50%. In **SF0.33-L** (**Fig. 6(g)**)with half bar ratio, the maximum strength V_{test} and lateral drift were decreased: +309 and -534 kN at the drift ratios of +0.45 and -0.20%. Unlike the specimens with h_w/l_w= 0.5, the safety margin of shear friction predictions were similar, regardless of the bar ratio: V_{test}/V_{sf} =0.71 and 0.69 in **SF0.33** and **SF0.33-L**, respectively.

In **SF0.33D** and **SF0.33D-L** (**Figs. 6(h)** and **(i)**) using additional shear friction reinforcement (f_{ysf}= 620 MPa, ρ_{sf}=0.38% in **SF0.33D**, and ρ_{sf} =0.24% in **SF0.33D-L**), the maximum strength V_{test} and lateral drift were significantly increased: in **SF0.33D** (maximum shear bar ratio), +1060 and -1031 kN at the drift ratio of +0.75 and -0.60%, and in **SF0.33D-L** (a half of the maximum shear bar ratio), +708 and -743 kN at the drift ratio of +1.0 and -0.60%. However, the test strength did not reach the ACI 349 shear friction strength: V_{test}/V_{sf} = 0.78 and 0.83 in **SF0.33D** and **SF0.33D-L**, respectively.

3.3 **Strains of web bars**

Fig. 6 shows strain distributions of the horizontal bars along the wall height at $0.5V_{max}$, $0.75V_{max}$, and $1.0V_{max}$. The locations of the bars and strain gauges are shown in the figure. In all specimens, yielding of the horizontal bars did not occur.

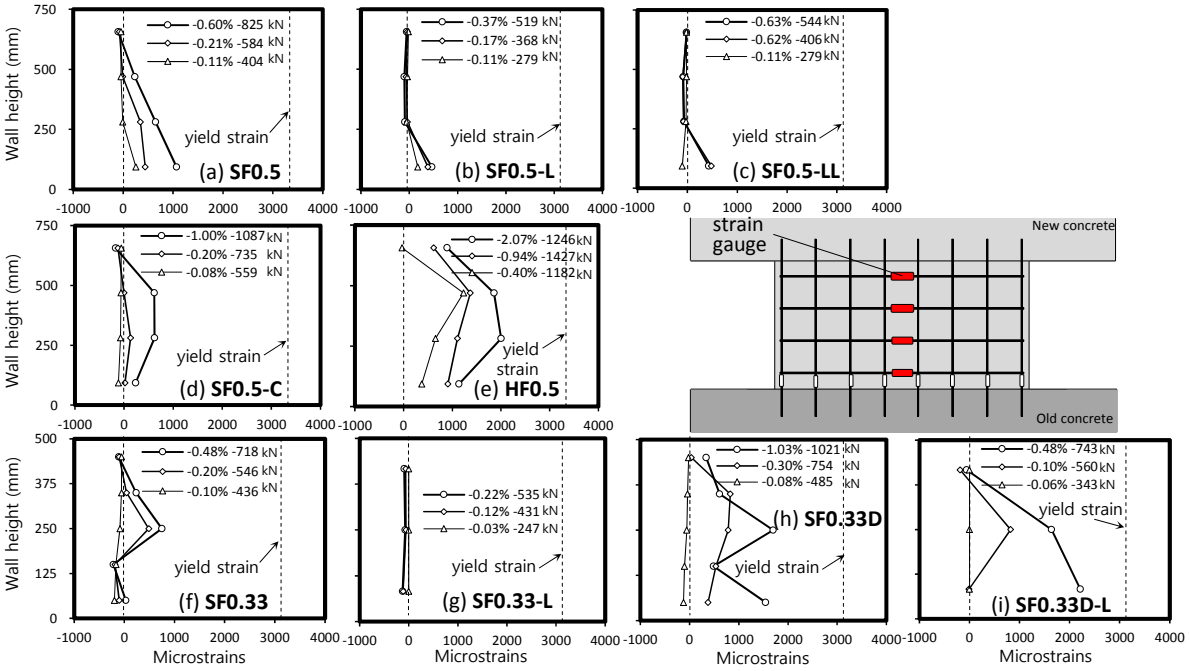

Figure 6. Measured strains of horizontal bars

In **HF0.5** where sliding failure did not occur, the horizontal bar strains were the greatest. In other specimens which failed due to sliding (**SF0.5**, **SF0.5-L**, **SF0.5-LL**, **SF0.5-C**, **SF0.33**, and **SF0.33-L**), the strains of the horizontal bars were extremely small, which indicates that the load-carrying capacity was limited by premature sliding failure.

In **SF0.33D** and **SF0.33D-L** with shear friction bars, the bar strain increased as the load-carrying capacity increased.

Fig. 7 shows strain distributions of the vertical web bars at $0.5V_{max}$, $0.75V_{max}$, and $1.0V_{max}$. The locations

of the bars and strain gauges are shown in the figure. In the figure, the strains were significantly less than the yield strain, which did not agree with the assumption of the ACI 349 shear friction design. This result indicates that the concept of shear friction design needs to be changed in the case of walls subjected to cyclic lateral loading.

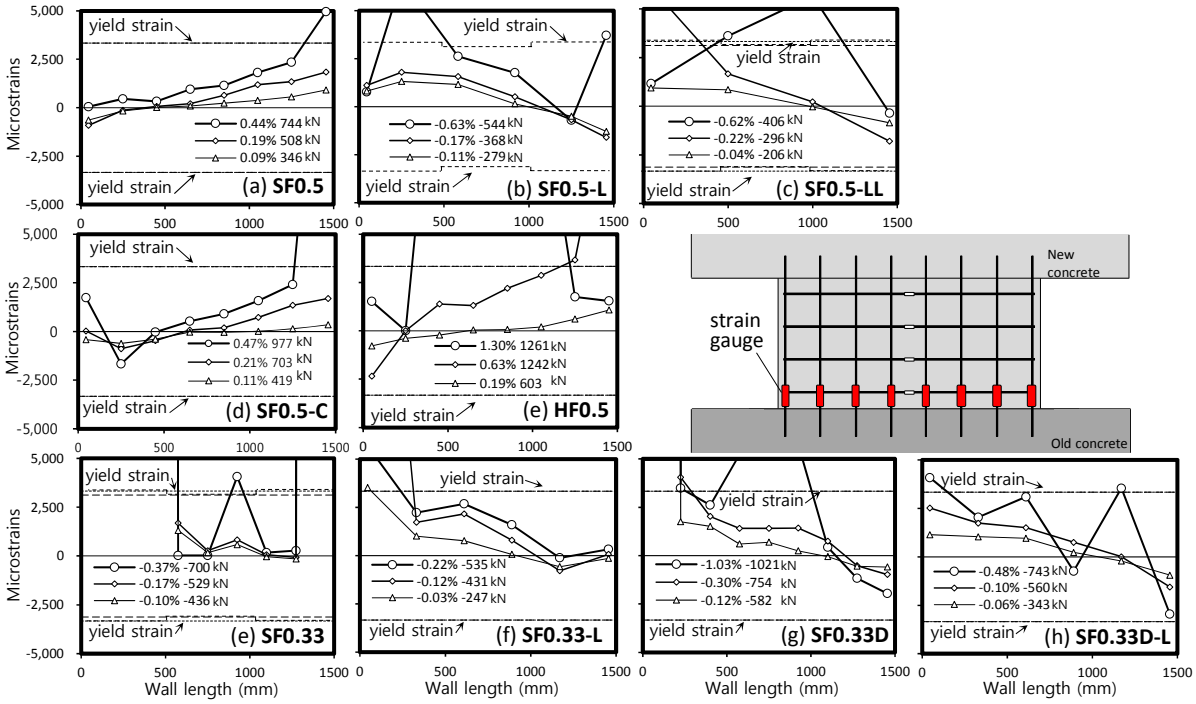

Figure 7. Measured strains of vertical bars

4 RECOMMENDATION FOR SHEAR FRICTION DESIGN WITH GRADE 550 MPA BARS

On the basis of test results, provisional recommendation for shear friction design with Grade 550 MPa bars were made as follows:

1. In walls without construction joints (μ = 1.4), design yield strength of 550MPa (actual yield strength = 667MPa) can be used for shear friction bars. However, in the construction of massive walls, the use of construction joints is inevitable.
2. In walls with construction joints (μ = 0.6), the design yield strength of shear friction bars needs to be limited to 420MPa (When 550MPa bars are used for vertical and horizontal bars, 550MPa can be used for shear design and flexural design, but for shear friction design, the design yield strength should be limited to 420MPa). However, the safety margin of shear friction design is relatively low when compared to the design shear strength or design flexural strength. Thus, shear friction failure may precede other failure modes.
3. When additional shear friction bars are necessary, the additional shear friction bars should not be terminated at the lower part of walls, but be extended to the upper part. Otherwise, premature shear friction failure can occur at the ends of the bars.

5 CONCLUSION

To investigate the shear friction capacity of walls with Grade 550 MPa web bars, five specimens with aspect ratio h_w/l_w =0.5 and four specimens with aspect ratio h_w/l_w =0.33 were tested under cyclic lateral loading. The major findings of the present study are summarized as follows:

1. In the walls where construction joint at the wall-foundation interface, the test strength did not reach the shear friction strength of ACI 349 (or ACI 318) and Eurocode 2. In the case of walls without shear friction bars, the test strength was 65 ~ 83% of the ACI 349 shear friction strength.
2. In the case of walls with shear friction bars, the shear friction bars increased the maximum strength, but the maximum strength did not reach the shear friction strength. The test strength was 78 ~ 83% of the ACI 349 shear friction strength.
3. In the case of walls subjected to axial compression, the test strength increased, but did not reach the shear-friction prediction. The test strength was 81% of the ACI 349 shear friction strength.
4. On the other hand, in the walls with groove construction joint, the test strength reached the wall shear strength, without shear friction failure.
5. Provisional recommendation for shear friction design with Grade 550 MPa bars were made on the basis of the test results. However, further studies are required considering other parameters of bar grade (420 MPa bars), roughened surface (μ=1.0), and size effect (larger bar diameter).

6 ACKNOWLEDGMENT

This work was supported by the Nuclear Power Core Technology Development Program of the Korea Institute of Energy Technology Evaluation and Planning (KETEP), granted financial resource from the Ministry of Trade, Industry & Energy, Republic of Korea (No. 2014151010169B).

REFERENCES:

Park, H.; Baek, J.; Lee, J., and Shin, H., "Cyclic Loading Tests for Shear Strength of Low-Rise Reinforced Concrete Walls with Grade 550 MPa Bars," *ACI Structural Journal*, 2015, **112**(3): pp. 299-310.

H., Kent A.; Z., Gabriel, and S., Bahram, "Toward an improved understanding of shear-friction behavior," *ACI Structural Journal*, 2012, **109**(6): pp. 835-844.

ACI Committee 349, "*Code Requirements for Nuclear Safety-Related Concrete Structures (ACI 349-13) and Commentary*," 2014: Farmington Hills, 200 pp.

ACI Committee 318, "*Building Code Requirements for Structural Concrete (ACI 318-14) and Commentary*," Farmington Hills, 2014, 520 pp.

Hawkins, NM, and Ghosh, SK, "Acceptance Criteria for Special Structural Walls Based on Validation Testing", 2003, *Proposed Provisional Standard and Commentary*, SK Ghosh Associates Inc., Northbrook, IL.